

ural site of action. This activity is specific to Int-6 because Tax does not alter the POD structure, as shown by examination of PML localization in the presence of Tax. Further analyses will determine not only the importance of the interaction in the onset of adult T cell leukemia in patients infected with HTLV-I but also a possible role of Int-6 in human nonviral cancers.

REFERENCES AND NOTES

1. B. J. Poiesz *et al.*, *Proc. Natl. Acad. Sci. U.S.A.* **77**, 7415 (1980); M. Yoshida, I. Miyoshi, Y. Hinuma, *ibid.* **79**, 2031 (1982); A. Gessain *et al.*, *Lancet* **ii**, 407 (1985); M. Osame *et al.*, *ibid.* **i**, 1031 (1986).
2. M. Nerenberg, S. H. Hinrichs, R. K. Reynolds, G. Khoury, G. Jay, *Science* **237**, 1324 (1987); R. Grassmann *et al.*, *Proc. Natl. Acad. Sci. U.S.A.* **86**, 3351 (1989); A. Tanaka *et al.*, *ibid.* **87**, 1071 (1990); R. Pozzatti, J. Vogel, G. Jay, *Mol. Cell. Biol.* **10**, 413 (1990).
3. P. Sarnow, Y. S. Ho, J. Williams, A. J. Levine, *Cell* **28**, 387 (1982); B. A. Werness, A. J. Levine, P. M. Howley, *Science* **248**, 76 (1990); J. A. DeCaprio *et al.*, *Cell* **54**, 275 (1988); P. Whyte *et al.*, *Nature* **334**, 124 (1988); N. Dyson, P. M. Howley, K. Münger, E. Harlow, *Science* **243**, 934 (1989).
4. S. Fields and O.-K. Song, *Nature* **340**, 245 (1989).
5. T. Durfee *et al.*, *Genes Dev.* **7**, 555 (1993).
6. We used the MATCHMAKER two-hybrid system (Clontech, Palo Alto, CA). The Tax coding sequence was fused to the GAL4 DNA binding domain into the pGB-T9 yeast expression vector, giving pGB-Tax. The human cDNA library we used has been described (5). Briefly, cDNAs from EBV-transformed human peripheral lymphocytes were fused to the GAL4 transcriptional activation domain into the  $\lambda$ ACT phage vector. pGB-Tax was introduced into the HF7c yeast strain, and the resulting cells were transformed by the fusion cDNA library. The HF7c strain possesses the His synthetase gene (*HIS3*) and the *lacZ* gene under the control of GAL4 binding sites. From an initial screen of 250,000 transformants, 700 were found to grow on a minimal medium lacking His. Of these, 94 were also positive when assayed for  $\beta$ -galactosidase expression. Plasmid DNAs from the double positive clones were extracted and sequenced.
7. A. Marchetti *et al.*, *J. Virol.* **69**, 1932 (1995).
8. C. Caron *et al.*, *EMBO J.* **12**, 4269 (1993).
9. Forty hours after transfection by the calcium phosphate precipitation method, cells were fixed for 15 min in 4% paraformaldehyde, followed by 20 min in 0.1 M glycine, and permeabilized for 5 min in 0.5% Triton X-100. Cells were then incubated for 1 hour with the monoclonal antibody M2 (Kodak) directed against the FLAG epitope or Tax antiserum. After washing, cells were further incubated for 45 min with appropriate secondary antibodies conjugated with fluorescein or rhodamine. Finally, nuclei were stained with Hoechst 33258.
10. M. Sugawara, T. Scholl, P. D. Ponath, J. L. Strominger, *Mol. Cell. Biol.* **14**, 8438 (1994).
11. C. Desbois, R. Rousset, F. Bantignies, P. Jalilnot, data not shown.
12. C. A. Ascoli and G. G. Maul, *J. Cell Biol.* **112**, 785 (1991).
13. P. Kastner *et al.*, *EMBO J.* **11**, 629 (1992).
14. J. A. Dyck *et al.*, *Cell* **76**, 333 (1994).
15. K. Weiss *et al.*, *ibid.*, p. 345.
16. Immunofluorescence experiments were performed as described for Fig. 3. Cells were examined with a confocal laser microscope (Zeiss). Fluorescein was excited at 488 nm, and rhodamine, at 543 nm. The two channels were recorded independently. Pseudocolor images were generated and superimposed with Photoshop software.
17. A. Kakizuka *et al.*, *Cell* **66**, 663 (1991); H. de Thé *et al.*, *ibid.*, p. 675; A. D. Goddard, J. Borrow, P. S. Freemont, E. Solomon, *Science* **254**, 1371 (1991); P. P. Pandolfi *et al.*, *Oncogene* **6**, 1285 (1991).

18. M. H. Koken *et al.*, *EMBO J.* **13**, 1073 (1994).
19. B. Terris *et al.*, *Cancer Res.* **55**, 1590 (1995).
20. U. M. Moll, G. Riou, A. J. Levine, *Proc. Natl. Acad. Sci. U.S.A.* **89**, 7262 (1992).
21. HeLa cells ( $0.7 \times 10^6$ ) were transfected by the calcium phosphate precipitation method with 1  $\mu$ g of the pG4G3CAT reporter construct (8), 10 ng of pG4M or pSG4-Tax (8), and 100 ng of pSG-FNV or pSG-FNV-70. pSG-FNV is a pSG5 derivative encoding the FLAG epitope fused to the SV40 nuclear localization signal and to the VP16 activation domain (amino acids 403 to 479). The clone 70 Int-6 cDNA was inserted into this parental plasmid to give pSG-FNV-70. Duplicate transfections were done for each combination of plasmids. Forty hours after transfection, concentrations of the CAT protein were measured by enzyme-linked immunosorbent assay (Boehringer Mannheim).
22. S. M. Hanly *et al.*, *Genes Dev.* **3**, 1534 (1989).
23. Complementary DNA from the Int-6 clone 88 was inserted in-frame with the FLAG epitope into pSG5, giving pSGF-Int-6. COS7 cells ( $0.7 \times 10^6$ ) were transfected with 1  $\mu$ g of pSGF-Int-6 or 1  $\mu$ g of pSG-Tax, or both. Cells were lysed in radioimmunoprecipitation assay buffer. The immunoprecipitates were separated on a 10% polyacrylamide-SDS gel and blotted onto nitrocellulose. The enhanced

- chemiluminescent detection system (ECL, Amersham) was used to visualize bound antibodies.
24. We generated a polyclonal rabbit antiserum to a peptide corresponding to the COOH-terminal 20 amino acids of Int-6 coupled to ovalbumin. To purify this serum, we produced a FLAG-Int-6 fusion protein in bacteria and coupled it to a FLAG M2 antibody affinity gel (Kodak). Covalent linkage between the protein and the M2 antibody was performed by treatment with glutaraldehyde. The antiserum to Int-6 was incubated with this matrix, and specific antibodies were eluted with 100 mM glycine (pH 2.5).
25. N. Stuurman *et al.*, *J. Cell Sci.* **101**, 773 (1992); G. G. Maul, E. Yu, A. M. Ishov, A. L. Epstein, *J. Cell. Biochem.* **59**, 498 (1995).
26. We thank S. Elledge for providing the cDNA library; B. Cullen for the antiserum to Tax; A. Dejean for the PML rabbit polyclonal serum; R. van Driel for the PML monoclonal antibody; P. Chambon for the PML expression vector; C. Souchier for help with confocal microscopy; F. Chatelet for assistance in preparing the figures; and J. Maryanski for critical reading of the manuscript. This work was supported by the Agence Nationale de Recherches sur le Sida and the Association pour la Recherche contre le Cancer (F.B.).

25 March 1996; accepted 25 June 1996

## Activation of the Budding Yeast Spindle Assembly Checkpoint Without Mitotic Spindle Disruption

Kevin G. Hardwick,\* Eric Weiss,\* Francis C. Luca, Mark Winey, Andrew W. Murray†

The spindle assembly checkpoint keeps cells with defective spindles from initiating chromosome segregation. The protein kinase Mps1 phosphorylates the yeast protein Mad1p when this checkpoint is activated, and the overexpression of Mps1p induces modification of Mad1p and arrests wild-type yeast cells in mitosis with morphologically normal spindles. Spindle assembly checkpoint mutants overexpressing Mps1p pass through mitosis without delay and can produce viable progeny, which demonstrates that the arrest of wild-type cells results from inappropriate activation of the checkpoint in cells whose spindle is fully functional. Ectopic activation of cell-cycle checkpoints might be used to exploit the differences in checkpoint status between normal and tumor cells and thus improve the selectivity of chemotherapy.

The spindle assembly checkpoint keeps cells with spindle defects from segregating their chromosomes. The defects the checkpoint detects include the absence of spindle microtubules (1, 2), monopolar spindles (3), and the misalignment of a single chromosome on the spindle (4). Mutations in the budding yeast *MAD* (mitotic arrest defective) (2) or *BUB* (budding uninhibited by benzimidazole) (1) genes inactivate the checkpoint and allow cells with defective spindles to proceed through mitosis. Another

checkpoint component, the essential protein kinase Mps1p (5, 6), has two roles in the cell cycle; it is required for spindle pole body duplication in G<sub>1</sub> (7) and for the spindle assembly checkpoint in mitosis (3). We found that Mps1p directly phosphorylated Mad1p and that overexpression of Mps1p constitutively activated the spindle assembly checkpoint in wild-type cells.

Spindle depolymerization causes hyperphosphorylation of Mad1p that leads to a decrease in the protein's gel mobility during SDS-polyacrylamide gel electrophoresis (PAGE) (8). To determine whether spindle pole body defects also induced this modification, we examined the phosphorylation of Mad1p at 37°C in *cdc31*, *mgs2*, and *mgs1* mutants, which are all defective in spindle pole body duplication (7, 9). The *cdc31* and *mgs2* mutants, which induce mitotic arrest,

K. G. Hardwick and A. W. Murray, Department of Physiology, University of California, San Francisco, CA 94143-0444, USA.

E. Weiss, F. C. Luca, M. Winey, Department of Molecular, Cellular, and Developmental Biology, University of Colorado, Boulder, CO 80309-0347, USA.

\*These authors contributed equally to this work.

†To whom correspondence should be addressed.

also cause increased phosphorylation of Mad1p (Fig. 1A). In contrast, no modification of Mad1p was detected in *mps1* cells, which failed to arrest at restrictive temperatures even when the cells were treated with nocodazole to induce microtubule depolymerization (3). These results link the hyperphosphorylation of Mad1p (8) with the role of Mps1p in the spindle assembly checkpoint (3) and suggest that modification of Mad1p is an essential step in the activation of the spindle assembly checkpoint.

To test whether Mps1p directly phosphorylates Mad1p, we used *in vitro* kinase assays with purified components. Active Mps1p was purified from yeast as a glutathione *S*-transferase (GST)–Mps1p fusion protein, and the NH<sub>2</sub>-terminal third of Mad1p was expressed and purified from *Escherichia coli*. Mps1p directly phosphorylated Mad1p (Fig. 1B), and this *in vitro* phosphorylation led to reduced mobility of Mad1p, as seen *in vivo* upon checkpoint activation (10). It remains to be determined whether this modification is required for the activation of the checkpoint.

To determine whether increasing the ac-

tivity of Mps1p would lead to Mad1p phosphorylation and mitotic arrest in cells whose spindle was normal, we overexpressed the *MPS1* gene by fusing it to the galactose-inducible *GAL1-10* promoter. We exposed cells transformed with this construct to galactose and monitored their spindle morphology by both light microscopy and electron microscopy (EM). Overexpression of Mps1p led to a cell-cycle arrest with a G<sub>2</sub> DNA content. These cells contained short bipolar spindles whose length and overall appearance when observed by EM were no different from those of normal mitotic cells that had not initiated anaphase B (Fig. 2) (11). Transfer of the mitotically arrested cells from galactose to glucose allowed them to complete mitosis and produce viable progeny, which showed that overexpression of Mps1p did not induce permanent spindle damage.

Overexpression of Mps1p could arrest the cell cycle by three different mechanisms: (i) activation of the spindle assembly checkpoint without impairment of spindle function, (ii) activation of the checkpoint by induction of spindle defects, or (iii) activation of a pathway that does not involve the checkpoint. To distinguish among these

possibilities, we overexpressed Mps1p in wild-type cells and in *mad1*, *mad2*, *mad3*, *bub1*, *bub2*, and *bub3* mutants and analyzed cell-cycle progression by pedigree analysis of individual cells growing on solid medium or by monitoring cell morphology and the amount of a mitotic cyclin, Clb2p, in cell populations in liquid culture. All of the mutants failed to arrest, which demonstrated that Mps1p overexpression arrests wild-type cells by activating the MAD- and BUB-dependent checkpoint (Fig. 3).

The *mad3*, *bub1*, *bub2*, and *bub3* mutants that overexpressed Mps1p produced viable progeny. In contrast, *mad1* and *mad2* cells that passed through mitosis with high concentrations of Mps1p produced dead progeny (Fig. 3). This lethality may be due to interference with spindle pole body duplication: Mps1p overexpression that was temporally restricted so that it did not overlap with the period of spindle pole body duplication still induced a mitotic arrest in wild-type cells but did not induce lethality in *mad1* or *mad2* cells. (12). The viability of the dividing *mad* and *bub* cells shows that Mps1p overexpression activates the spindle assembly checkpoint without producing defects that interfere with chromosome segre-

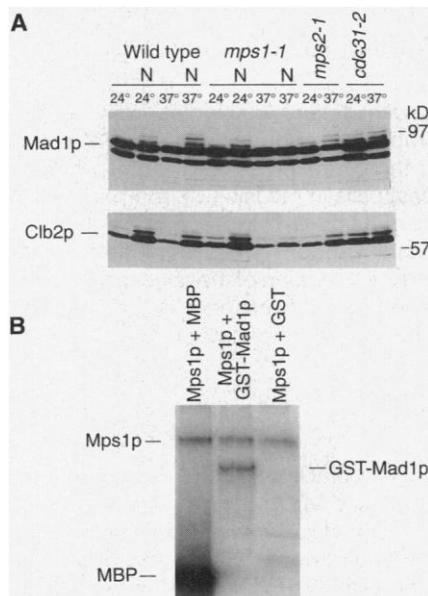


**Fig. 1.** Mad1p phosphorylation induced in cells arrested with monopolar spindles, and by the Mps1 kinase *in vitro*. (A) Immunoblot of Mad1p and the mitotic cyclin Clb2p in total cell lysates made from wild-type, *mps1*, *mps2*, and *cdc31* strains grown at permissive (24°C) and restrictive (37°C) temperatures. Wild-type and *mps1* strains were grown either in the presence or absence of the microtubule-destabilizing drugs benomyl and nocodazole (N). In all conditions where cells were arrested, Mad1p was phosphorylated and an accumulation of Clb2p was seen (22). (B) Mps1 kinase autophosphorylated and phosphorylated a Mad1–GST fusion protein and MBP, but did not phosphorylate GST, in an *in vitro* kinase assay (23).

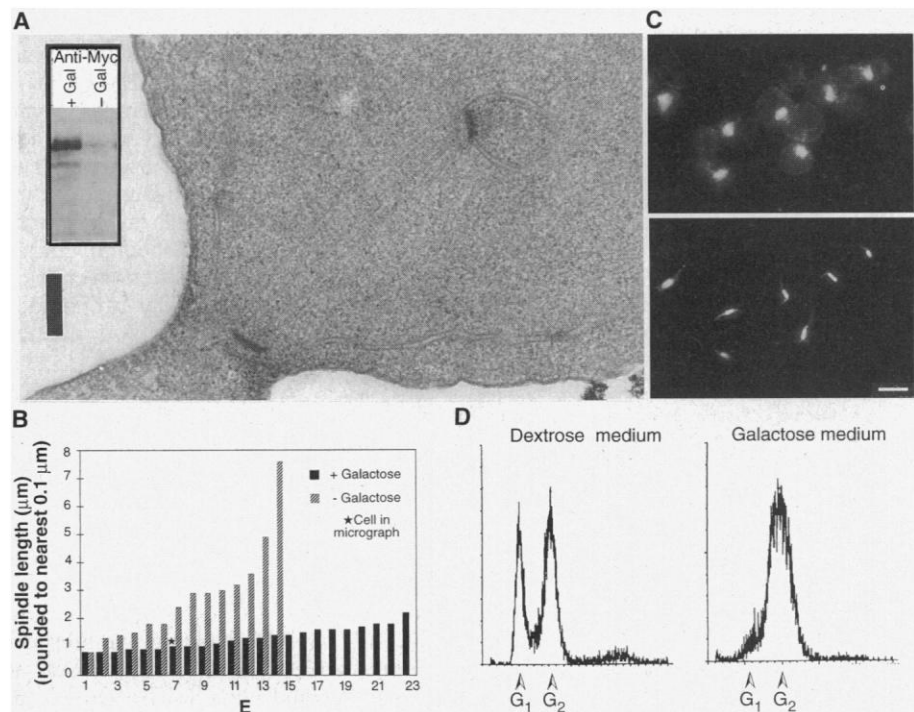


**Fig. 2.** Cell cycle arrest and spindle morphology in cells overexpressing Mps1p. (A) Overexpression of Mps1p tagged with the Myc epitope (inset) did not affect mitotic spindle structure as seen in the EM but did arrest cells with nearly uniform spindle lengths. Anti-Myc denotes the antigen to the Myc protein. (B) Each bar in graph represents an individual budded cell. (C) Light microscopy of cell populations overexpressing Mps1p revealed large budded cells, with short spindles as detected by tubulin immunofluorescence (bottom) and unsegregated DNA masses as revealed by 4',6'-diamidino-2-phenylindole staining (top). (D) The DNA content of the galactose-treated cells was 2C (right); untreated cells with wild-type amounts of Mps1p had a normal distribution of DNA contents (left) (24). Bar, 0.2 μm (A) and 5 μm (C).

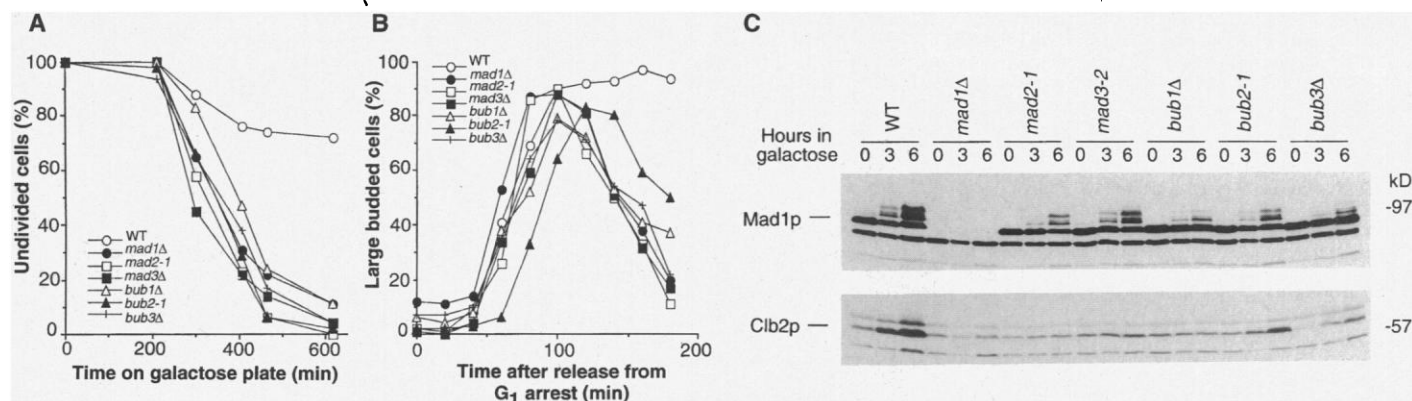


**Fig. 3.** Failure of overexpression of *MPS1* to arrest *mad* and *bub* strains, even though Mad1p was hyperphosphorylated. The graphs depict microcolony assays (**A**) and budding index in liquid cultures (**B**) of the indicated strains. Certain mutants died as a result of the mitotic divisions [strain viability

in (**A**): wild type (WT), 94%; *mad1Δ*, 9%; *mad2-1*, 17%; *mad3Δ*, 94%; *bub1Δ*, 72%; *bub2-1*, 92%; and *bub3Δ*, 88%]. (**C**) Immunoblots of Mad1p show that none of the known Mad or Bub proteins are necessary for Mad1p modification when *MPS1* is overexpressed (25).

gation. Wild-type cells eventually adapt to continued overexpression of Mps1p and divide and form viable colonies on plates containing galactose.

To strengthen the correlation between Mad1p modification and activation of the spindle assembly checkpoint, we analyzed the modification of Mad1p in cells overexpressing Mps1p. Mad1p was hyperphosphorylated in wild-type cells and in all of the *mad* and *bub* mutants except *mad1Δ* (Fig. 3C). The observation that none of the known Mad or Bub proteins are required for Mps1 overexpression to increase phosphorylation of Mad1p in vivo supports the hypothesis that Mad1p is a physiological substrate of Mps1p.

In cells with wild-type amounts of Mps1p, the presence of Bub1p and Bub3p is required for the increased phosphorylation of Mad1p induced by microtubule depolymerization (8), which suggests that Bub1p [which has protein kinase activity (13)] and Bub3p may be required for the activation of Mps1p. In cells overexpressing Mps1p, however, Bub1p and Bub3p are not needed for Mad1p modification, although they are required to induce cell-cycle arrest. These results suggest that the requirements for the modification of Mad1p are complex and show that the phosphorylation of Mad1p induced by overexpression of Mps1p is not sufficient to induce cell-cycle arrest. Despite these complexities, our results suggest that Mps1p may be a physiologically important Mad1p kinase whose activity is required to detect a wide variety of spindle defects.

Many humans and rodent tumors have defects in cell-cycle checkpoints (14). Inactivation of the p53 tumor suppressor gene impairs the cell's ability to prevent the onset of DNA replication when DNA damage occurs and increases genetic instability (15). Loss of p53 function also impairs the

spindle assembly checkpoint (16) and the normal regulation of centrosome duplication (17). These observations indicate that, like Mps1p, the p53 protein may participate in both control of microtubule organizing center duplication and the checkpoint that assesses spindle function.

We have shown that a genetic manipulation of a cell-cycle checkpoint, the overexpression of Mps1p, can arrest undamaged wild-type cells but not checkpoint-defective cells. This finding has potential therapeutic applications. Constitutively activating a checkpoint could arrest normal cells and allow selective killing of checkpoint-defective tumor cells by cytotoxic treatments that kill cells passing through the cell cycle. Constitutive activation of checkpoint components could kill certain checkpoint defective mutants, such as Mps1p overexpression kills the *mad1* and *mad2* mutants.

## REFERENCES AND NOTES

- M. A. Hoyt, L. Totis, B. T. Roberts, *Cell* **66**, 507 (1991).
- R. Li and A. W. Murray, *ibid.*, p. 519.
- E. Weiss and M. Winey, *J. Cell Biol.* **132**, 111 (1996).
- X. Li and R. B. Nicklas, *Nature* **373**, 630 (1995); C. L. Rieder, R. W. Cole, A. Khodjakov, G. Sluder, *J. Cell Biol.* **130**, 941 (1995); W. A. E. Wells and A. W. Murray, *ibid.* **133**, 75 (1996).
- O. Poch *et al.*, *Mol. Gen. Genet.* **243**, 641 (1994).
- E. Lauze *et al.*, *EMBO J.* **14**, 1655 (1995).
- M. Winey, L. Goetsch, P. Baum, B. Byers, *J. Cell Biol.* **114**, 745 (1991).
- K. G. Hardwick and A. W. Murray, *ibid.* **131**, 709 (1995).
- B. Byers, in *The Molecular Biology of the Yeast Saccharomyces: Life Cycle and Inheritance*, J. N. Strathern, E. W. Jones, J. R. Broach, Eds. (Cold Spring Harbor Laboratory, Cold Spring Harbor, NY, 1981), pp. 59–96.
- K. G. Hardwick, unpublished data.
- M. Winey *et al.*, *J. Cell Biol.* **129**, 1601 (1995).
- K. G. Hardwick, unpublished data.
- R. T. Roberts, K. A. Farr, M. A. Hoyt, *Mol. Cell. Biol.* **14**, 8282 (1994).
- L. H. Hartwell and M. B. Kastan, *Science* **266**, 1821 (1994).
- L. R. Livingstone *et al.*, *Cell* **70**, 923 (1992).
- S. M. Cross *et al.*, *Science* **267**, 1353 (1995).
- K. Fukasawa, T. Choi, R. Kuriyama, S. Rulong, G. F. Vande Woude, *ibid.* **271**, 1744 (1996).
- D. A. Mitchell, T. K. Marshall, R. J. Deschenes, *Yeast* **9**, 715 (1993).
- G. I. Evan, G. K. Lewis, G. Ramsey, J. M. Bishop, *Mol. Cell. Biol.* **5**, 3610 (1985).
- B. Byers and L. Goetsch, *Methods Enzymol.* **194**, 608 (1991).
- K. J. Hutter and H. E. Eipel, *J. Gen. Microbiol.* **113**, 369 (1979).
- Cells were grown in rich growth medium [yeast extract, peptone, and dextrose (YPD)] for 3 hours at the indicated temperatures (Fig. 1). Nocodazole was used at 20  $\mu$ g/ml in combination with benomyl at 30  $\mu$ g/ml. Both drugs were necessary to maintain the arrest in wild-type cells at 37°C. Cell lysates were prepared, and immunoblotting was done as described (8). Strains are wild type (KH146), *mps1-1* (WX241-2b), *mps2-1* (WX178-3c), and *cdc31-2* (ELW65-9b). The *cdc31* cells exhibited delayed mitosis even when grown at 24°C.
- Mps1p was purified as a GST-fusion protein from yeast cells (6), and the GST was removed by cleavage with thrombin (18). Mad1-GST fusion proteins were purified and dialyzed as described (8). Kinase reaction conditions were as described (6) with the addition of approximately 18 nM GST-Mad1p, GST, or myelin basic protein (MBP). All substrates were present in Coomassie blue-stainable quantities. This Mad1-GST fusion contained residues 27 through 310 of Mad1p. A COOH-terminal fragment of Mad1p (residues 593 through 749) was also phosphorylated in this assay (12).
- Mps1p overexpression was achieved by placing the *MPS1* gene behind the *GAL10* promoter on a 2- $\mu$ m plasmid (Fig. 2A). A single myc epitope was inserted with custom oligonucleotides into a Not I site that had been engineered by inserting linkers into a Hinc II site that follows the second codon of the *MPS1* open reading frame. To create pELW325 [2  $\mu$ m, *LEU2*, *GAL10-NmycMPS1*], we inserted the NH<sub>2</sub>-terminally myc-tagged *MPS1* gene in an Afl III to Sma I fragment into pNZ2 digested with Nco I and Sma I. The pELW325 was then transformed into yeast strain BJ2168, and galactose-driven overexpression of Mps1p was confirmed by immunoblotting with the 9E10 antibody (19) (Fig. 2A, inset). Cells (ELW175) grown in medium containing 2% raffinose or exposed to 3% galactose for 6 hours were prepared for EM (20) and viewed on a Philips CM10 microscope (Mahwah, NJ). Spindle lengths were measured from spindle pole body to spindle pole body directly on the negatives from the EM and corrected for magnification (Fig. 2B). Several spindles traversed serial sections and required spindle length correction for section thickness (70 to 80 nm) by triangulation. KH135 cells (which contain pAFS120, a *GAL1-Nmyc*

*MPS1* integration construct made by polymerase chain reaction to introduce Xho I and Eco RI sites at either end of the *NmycMPS1* fragment, allowing it to be subcloned into pDK20) were grown overnight in yeast-extract peptone (YEP) containing 2% raffinose, arrested by exposure to 4% galactose for 5 hours, and prepared for immunofluorescence as described (Fig. 2C) (8). ELW200 cells (integrated *GAL1-NmycMPS1*) were grown in YEP containing 2% dextrose or shifted into YEP with 3% galactose for 6 hours and prepared for flow cytometry as described (Fig. 2D) (21). The DNA stained by propidium iodide in 5000 cells per sample was detected on a Becton Dickinson FACScan flow cytometer.

25. Unbudded cells containing integrated copies of *GAL-MPS1* were picked individually and placed on slabs containing 4% galactose (Fig. 3A). The cells were grown at 30°C, and the number of cells that had divided and rebudded were counted at the times

shown. Each point is an average from at least 50 cells. Strains are wild type (KH153), *mad1Δ.1* (KH155), *mad2-1* (KH157), *mad3-2* (KH150), *bub1Δ* (KH161), *bub2-1* (KH163), and *bub3Δ* (KH165). Cells of the strains listed above were grown in YEP with 2% raffinose to mid-log phase, collected, and incubated in fresh medium for 90 min with the addition of alpha factor to a final concentration of 10 μM. The cells were collected and resuspended in YEP containing 2% raffinose, 10 μM alpha factor, and 3% galactose and incubated for 2 hours. Finally, cells were collected, rinsed once in medium without alpha factor, and released into YEP containing 2% raffinose and 3% galactose. Timing began at the release from mating factor arrest, and samples were taken every 20 min. Cells were fixed with 70% ethanol and examined microscopically to determine the fraction of large budded cells as described (3). Cells of the previously mentioned strains were grown overnight in YEP with 4% raffinose and then galactose was

added to a final concentration of 4%. Samples were taken after 3 and 6 hours of growth at 30°C. Control (0) cells were grown for 3 hours in dextrose (Fig. 3C). 26. We thank A. Straight for the integrating *GAL1-MPS1* construct, T. Giddings for help with the EM analysis, A. Hoyt and B. T. Roberts for *bub* strains and deletion constructs, and all the members of our labs for their advice and encouragement. pNZ2 was provided by G. N. Zecherle of the University of Washington, Seattle, and pDK20 was provided by D. Kellogg of the University of California, Santa Cruz. K.G.H. and F.C.L. are Fellows of the Leukemia Society of America and E.W.W. was a trainee of NIH. This work was supported by grants to A.W.M. from NIH, the March of Dimes, and the David and Lucile Packard Foundation; and to M.W. from NIH, the American Cancer Society, and the Pew Scholars Program in the Biomedical Sciences.

22 April 1996; accepted 24 June 1996

## Regulation of Cardiac $\text{Na}^+$ , $\text{Ca}^{2+}$ Exchange and $\text{K}_{\text{ATP}}$ Potassium Channels by $\text{PIP}_2$

Donald W. Hilgemann\* and Rebecca Ball

Cardiac  $\text{Na}^+$ ,  $\text{Ca}^{2+}$  exchange is activated by a mechanism that requires hydrolysis of adenosine triphosphate (ATP) but is not mediated by protein kinases. In giant cardiac membrane patches, ATP acted to generate phosphatidylinositol-4,5-bisphosphate ( $\text{PIP}_2$ ) from phosphatidylinositol (PI). The action of ATP was abolished by a PI-specific phospholipase C (PLC) and recovered after addition of exogenous PI; it was reversed by a  $\text{PIP}_2$ -specific PLC; and it was mimicked by exogenous  $\text{PIP}_2$ . High concentrations of free  $\text{Ca}^{2+}$  (5 to 20 μM) accelerated reversal of the ATP effect, and PLC activity in myocyte membranes was activated with a similar  $\text{Ca}^{2+}$  dependence. Aluminum reversed the ATP effect by binding with high affinity to  $\text{PIP}_2$ . ATP-inhibited potassium channels ( $\text{K}_{\text{ATP}}$ ) were also sensitive to  $\text{PIP}_2$ , whereas  $\text{Na}^+$ ,  $\text{K}^+$  pumps and  $\text{Na}^+$  channels were not. Thus,  $\text{PIP}_2$  may be an important regulator of both ion transporters and channels.

Cardiac  $\text{Na}^+$ ,  $\text{Ca}^{2+}$  exchange activity can be enhanced by several acidic lipids (1, 2) that may occur in domains in cell membranes (3). In cardiac membrane patches treated with ATP, acidic lipids are generated on the cytoplasmic side of the membrane in parallel with a stimulation of  $\text{Na}^+$ ,  $\text{Ca}^{2+}$  exchange current (2, 4). The underlying mechanism might be (i) an ATP-dependent transport of phosphatidylserine (PS) from the extracellular to the cytoplasmic side by an amino phospholipid "flippase" (5), (ii) the phosphorylation of diacylglycerol (DAG) to form phosphatidic acid (PA) (6), or (iii) the phosphorylation of PI to form PIP and  $\text{PIP}_2$  (7). We used specific phospholipases and phospholipid vesicles to modify the lipid composition of giant cardiac membrane patches (8) and determined that the major mechanism is the generation of  $\text{PIP}_2$  from PI.

Outward  $\text{Na}^+$ ,  $\text{Ca}^{2+}$  exchange current was increased by addition of Mg-ATP to the cytoplasmic side of inside-out giant cardiac membrane patches (Fig. 1A) (9). The current was first activated by application of 90 mM  $\text{Na}^+$  to the cytoplasmic side of the patch with 2 mM extracellular (pipette)  $\text{Ca}^{2+}$ . With the free cytoplasmic  $\text{Ca}^{2+}$  concentration used (0.5 μM) the current inactivated (decreased) by about 80% over 15 s. Subsequent application of Mg-ATP (2 mM) for 40 s increased the current sixfold, and after ATP was removed the current remained stimulated for 100 s, after which it was turned off by removal of  $\text{Na}^+$ .

The record in Fig. 1A is a control experiment from a randomized series of patches, one-half of which were treated for 4 min with a phospholipase C that specifically hydrolyzes PI (PI-PLC) (10). The PI-PLC treatment (0.6 U/ml) did not significantly decrease the current before application of ATP (11) (Fig. 1B), and PI-PLC had no effect after the current had been stimulated by ATP (12). However, the treatment decreased the ATP effect by 96% ( $P < 0.001$ ).  $\text{PIP}_2$  (50 μM) strongly activated the ex-

change current, although ATP did not (Fig. 1B). Pure PI vesicles (0.3 mM) were applied for 60 s to other treated patches that failed to respond to ATP (Fig. 1C). PI had no effect by itself, but it restored the capacity of ATP to stimulate the exchange current.

The effect of ATP was reversed by a recombinant  $\text{PIP}_2$ -specific phospholipase C, PLC-β1, that is fully activated by 0.5 μM free  $\text{Ca}^{2+}$  under standard assay conditions (Fig. 2A) (13). This PLC-β1 was histidine-tagged, expressed in Sf9 cells, purified by  $\text{Ni}^{2+}$ -chelate affinity chromatography, and dialyzed against the solution used in the experiments. Reversal of the ATP effect after ATP removal was very slow (Fig. 2A). However, upon application of PLC-β1 (0.2 mg ml<sup>-1</sup> with a maximal specific activity of 100 μmol min<sup>-1</sup> mg<sup>-1</sup>), the current declined to its original value within 40 s (in three similar experiments). PLC-β1 had no effect when it was applied to patches in which the exchange current had been stimulated by PS rather than ATP (12).

High concentrations of cytoplasmic free  $\text{Ca}^{2+}$  induced a fast reversal of the ATP effect, probably mediated by an endogenous  $\text{Ca}^{2+}$ -dependent PLC (Fig. 2B). After ATP was applied and removed, 20 μM free  $\text{Ca}^{2+}$  was applied. At first, the exchange current was slightly stimulated because cytoplasmic  $\text{Ca}^{2+}$  activates the exchanger by an intrinsic regulatory mechanism (14). Thereafter, the exchange current declined rapidly over 30 s, and it declined to below its original level when free  $\text{Ca}^{2+}$  was reduced back to 0.5 μM (15). To determine the  $\text{Ca}^{2+}$  dependence of endogenous cardiac membrane-associated PLC, a crude membrane fraction was prepared from guinea-pig myocytes, and PLC activity was measured as inositol trisphosphate ( $\text{IP}_3$ ) released from exogenous vesicles containing [<sup>3</sup>H] $\text{PIP}_2$  (16). The PLC activity of the cardiac membranes was slightly activated with 0.5 μM free  $\text{Ca}^{2+}$  and was maximally activated with 20 μM free  $\text{Ca}^{2+}$  (Fig. 2C), which correlates with the ability of 20

D. W. Hilgemann, Department of Physiology, University of Texas, Southwestern Medical Center at Dallas, Dallas, TX 75235-9040, USA.

R. Ball, Department of Pharmacology, University of Texas, Southwestern Medical Center at Dallas, Dallas, TX 75235-9041, USA.

\*To whom correspondence should be addressed.